Atmos. Meas. Tech. Discuss., https://doi.org/10.5194/amt-2017-403
Manuscript under review for journal Atmos. Meas. Tech.
Discussion started: 5 February 2018

Atmospheric Measurement Techniques Discussions

Monte Carlo method for determining uncertainty of total ozone derived from direct solar irradiance spectra: Application to Izaña results

Anna Vaskuri[1], Petri Kärhä[1], Luca Egli[2], Julian Gröbner[2], and Erkki Ikonen[1, 3]

[1]Metrology Research Institute, Aalto University, PO Box 15500, 00076 Aalto, Finland
[2]Physikalisch-Meteorologisches Observatorium Davos, World Radiation Center, Dorfstrasse 33, 7260 Davos Dorf, Switzerland
[3]MIKES Metrology, VTT Technical Research Centre of Finland Ltd, PO Box 1000, 02044 VTT, Finland

Correspondence to: Anna Vaskuri (anna.vaskuri@aalto.fi), Petri Kärhä (petri.karha@aalto.fi)

Abstract. We demonstrate a Monte Carlo model to calculate the uncertainties of total ozone column, TOC, derived from ground-based directional solar spectral irradiance measurements. The model takes into account effects that correlations in the spectral irradiance data may have on the results. The model is tested with spectral data measured with three different spectroradiometers at an intercomparison campaign of the research project "Traceability for atmospheric total column ozone" at Izaña, Tenerife on 17 September 2016. The TOC values derived at noon have expanded uncertainties of 1.3% for a high-end scanning spectroradiometer, 1.3% for a high-end array spectroradiometer, and 3.3% for a roughly adopted instrument based on commercially available components and an array spectroradiometer. The level of TOC measured with reference Brewer spectrophotometer #183 is of the order of 282 DU during the analysed day and in agreement with the results of the two former instruments.

1 Introduction

Total ozone column (TOC) can be determined from spectral measurements of direct solar ultraviolet (UV) irradiance (Huber *et al.* (1995)). We have developed a Monte Carlo (MC) based model to estimate the uncertainties of the derived TOC values. One frequently overlooked problem with uncertainty evaluation is that the spectral data may hide systematic wavelength dependent errors due to correlations (Kärhä *et al.* (2017b, 2018); Gardiner *et al.* (1993)). The reason often is that the correlations are not known. Omitting possible correlations may lead into underestimated uncertainties for derived quantities, since spectrally varying systematic errors typically produce larger deviations than uncorrelated noise-like variations that traditional uncertainty estimations predict. Accounting for increased uncertainties arising from the correlations improves reliability of observing and predicting long term environmental trends, such as changes in the stratospheric ozone concentration (e.g. Molina and Rowland (1974)) and solar UV radiation (e.g. Kerr and McElroy (1993); McKenzie *et al.* (2007)).

In this paper, we introduce a new method for dealing with possible correlations in spectral irradiance data and analyse uncertainties for three different spectroradiometers used in a recent intercomparison campaign at Izaña, Tenerife, to demonstrate how it can be used in practice. One of the instruments is the QASUME spectroradiometer (Gröbner *et al.* (2005))

Atmos. Meas. Tech. Discuss., https://doi.org/10.5194/amt-2017-403
Manuscript under review for journal Atmos. Meas. Tech.
Discussion started: 5 February 2018

Atmospheric Measurement Techniques Discussions

that serves as a high-quality reference instrument of spectral irradiance at PMOD/WRC. The second one is AVODOR, a simple array based spectrograph from Avantes, and the third one is BTS2048-30-UV-S-WP (BTS) from Gigahertz-Optik, an array-based high-quality spectrograph that has been optically corrected for stray light (Zuber *et al.* (2017a, b)), operated by PTB. The field of view of the spectroradiometers has been limited so that they measure directional irradiance of the Sun only, excluding the blue sky.

2 The Izaña field measurement campaign

Traceability for atmospheric total column ozone (ATMOZ) was a three-year research project funded by the EMRP program of the European Union in 2014 – 2017. The project arranged a field measurement campaign (ATMOZ campaign (2016)) that took place between 12 – 25 September 2016 at the Izaña Atmospheric Observatory in Tenerife, Canary Islands, Spain. The measurement campaign was organised by the Spanish Meteorological Agency (AEMET) and the World Radiation Center (PMOD/WRC) for the intercomparison of TOC measured with different participating instruments, including Dobson and Brewer spectrophotometers, and various spectroradiometers.

The focus of this paper is to study uncertainties of the TOC values derived from direct solar UV irradiance spectra. We study the data measured during the day of 17 September 2016 with three different spectroradiometers using the ozone retrieval algorithm introduced in Section 3. The measurements took place on the mountain Teide at the altitude of 2.36 km above the sea level (28.3090° N, 16.4990° W). Station pressure of 772.8 hPa was monitored during the campaign with a standard uncertainty of 1.3 hPa. The ozone and temperature profiles were measured with a sonde prior to measurements as shown in Fig. 1.

Atmos. Meas. Tech. Discuss., https://doi.org/10.5194/amt-2017-403
Manuscript under review for journal Atmos. Meas. Tech.
Discussion started: 5 February 2018

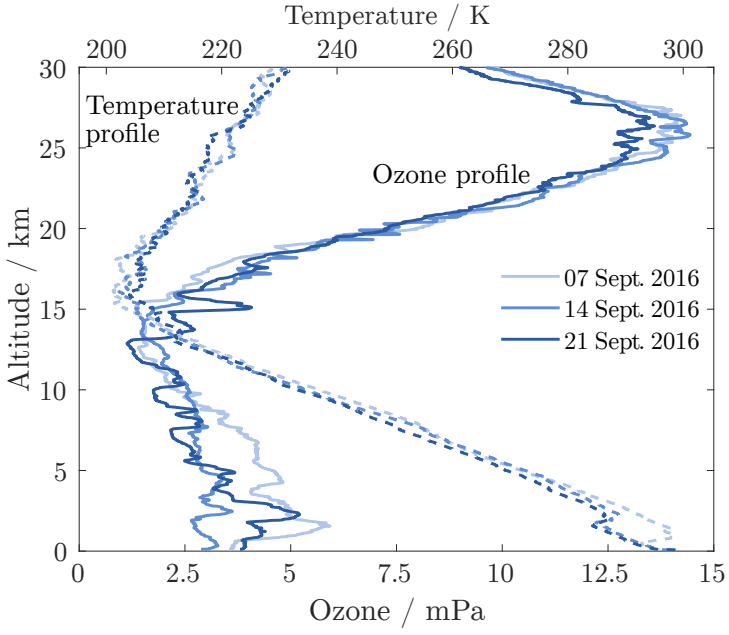

Figure 1. Temperature and ozone profiles as a function of the altitude, measured with a sonde during the ATMOZ field measurement campaign.

In our ozone retrieval, vertical profiles were not implemented in the model to reduce computational complexity, which may slightly shift the absolute values, but should not have an effect on the uncertainties obtained. With a one layer model, the ozone absorption cross-section is a function of the effective temperature and the relative air mass is a function of the effective altitude of the ozone layer. Using the vertical ozone profile $\rho_{O_3}(z)$, the effective altitude $h_{\text{eff}} = 26$ km ± 0.5 km of the ozone layer was estimated by integration over altitudes

$$h_{\text{eff}} = \frac{\int_{z_0}^{z_1} z\, \rho_{O_3}(z)\, \mathrm{d}z}{\int_{z_0}^{z_1} \rho_{O_3}(z)\, \mathrm{d}z}, \tag{1}$$

from the station altitude z_0 to the top-of-the-atmosphere altitude z_1. The corresponding effective temperature $T_{\text{eff}} = 228$ K ± 1 K was estimated (Komhyr *et al.* (1993); Fragkos *et al.* (2015)) as

$$T_{\text{eff}} = \frac{\int_{z_0}^{z_1} T(z)\, \rho_{O_3}(z)\, \mathrm{d}z}{\int_{z_0}^{z_1} \rho_{O_3}(z)\, \mathrm{d}z}. \tag{2}$$

The uncertainties stated for h_{eff} and T_{eff} are standard deviations.

The data sets measured by three different spectroradiometers were studied in this work. One of the instruments was the QASUME double-monochromator spectroradiometer (Gröbner *et al.* (2005)) of PMOD/WRC. The measurement range of QASUME during the campaign was limited to 250 nm – 500 nm with a step interval of 0.25 nm so that one spectrum could be measured every 15 minutes. The second one was AVODOR, a simple array based spectrograph from Avantes, with a step interval of 0.14 nm. The third one was an array-based spectrograph BTS from Gigahertz-Optik that has been optically corrected

Atmos. Meas. Tech. Discuss., https://doi.org/10.5194/amt-2017-403
Manuscript under review for journal Atmos. Meas. Tech.
Discussion started: 5 February 2018

Atmospheric Measurement Techniques Discussions

for stray light using an internal filter wheel (Zuber *et al.* (2017a, b)), operated by PTB. The measurement range of BTS was between 200 nm and 430 nm with a step interval of 0.2 nm during the campaign. Uncertainty components of the spectral measurements are listed in Table 1 for QASUME, in Table 2 for AVODOR, and in Table 3 for BTS spectroradiometers. The tables also give division of the uncertainty components to different correlation types as described in Section 4.

Table 1. Uncertainties of the measurement for QASUME spectroradiometer.

QASUME	Standard	Correlation		
Source of uncertainty	uncertainty	*full*	*unfavourable*	*random*
in measured $E(\lambda)$	%		Fraction	
Radiometric calibration	0.55	$1/\sqrt{3}$	$1/\sqrt{3}$	$1/\sqrt{3}$
250 W lamp stability	0.14	1	0	0
Non-linearity	0.25	0	1	0
Stability	0.60	1	0	0
Temperature dependence	0.20	1	0	0
Measurement noise	0.20	0	0	1
Wavelength shift	0.10	0	1	0
Combined uncertainty ($k = 1$)	0.91%	0.72%	0.42%	0.38%

Table 2. Uncertainties of the measurement for AVODOR spectroradiometer.

AVODOR	Standard	Correlation		
Source of uncertainty	uncertainty	*full*	*unfavourable*	*random*
in measured $E(\lambda)$	%		Fraction	
Radiometric calibration	2.50	1/2	1/2	$1/\sqrt{2}$
250 W lamp stability	0.14	1	0	0
Non-linearity	0.50	0	1	0
Stability	0.60	1	0	0
Temperature dependence	0.20	1	0	0
Measurement noise	1.30	0	0	1
Wavelength shift	0.10	0	1	0
Combined uncertainty ($k = 1$)	2.94%	1.41%	1.35%	2.19%

Atmos. Meas. Tech. Discuss., https://doi.org/10.5194/amt-2017-403
Manuscript under review for journal Atmos. Meas. Tech.
Discussion started: 5 February 2018

Atmospheric Measurement Techniques Discussions

Table 3. Uncertainties of the measurement for BTS spectroradiometer (Zuber *et al.* (2017b)).

BTS	Standard	Correlation		
Source of uncertainty	uncertainty	*full*	*unfavourable*	*random*
in measured $E(\lambda)$	%	Fraction		
Radiometric calibration	0.80	$1/\sqrt{3}$	$1/\sqrt{3}$	$1/\sqrt{3}$
250 W lamp stability	0.20	1	0	0
Non-linearity	0.40	0	1	0
Stability	0.80	1	0	0
Temperature dependence	0.10	1	0	0
Measurement noise	0.20	0	0	1
Wavelength shift	0.10	0	1	0
Combined uncertainty ($k = 1$)	1.24%	0.95%	0.62%	0.50%

The slit functions of the three spectroradiometers shown in Fig. 2 were measured with lasers before the measurement campaign. They are needed when fitting the ozone retrieval to the measured spectra. In addition, it is of importance to notice the different wavelength steps of the data, 0.25 nm for QASUME, 0.2 nm for BTS, and 0.14 nm for AVODOR. The wavelength steps of the spectral data affect the magnitudes of the uncertainties in TOC created by spectrally random components. The number of data points N which is smaller with a larger wavelength step interval, affects uncertainties with a factor of $\sqrt{N}$ as demonstrated in (Kärhä *et al.* (2017b)).

Atmos. Meas. Tech. Discuss., https://doi.org/10.5194/amt-2017-403
Manuscript under review for journal Atmos. Meas. Tech.
Discussion started: 5 February 2018

Atmospheric Measurement Techniques Discussions

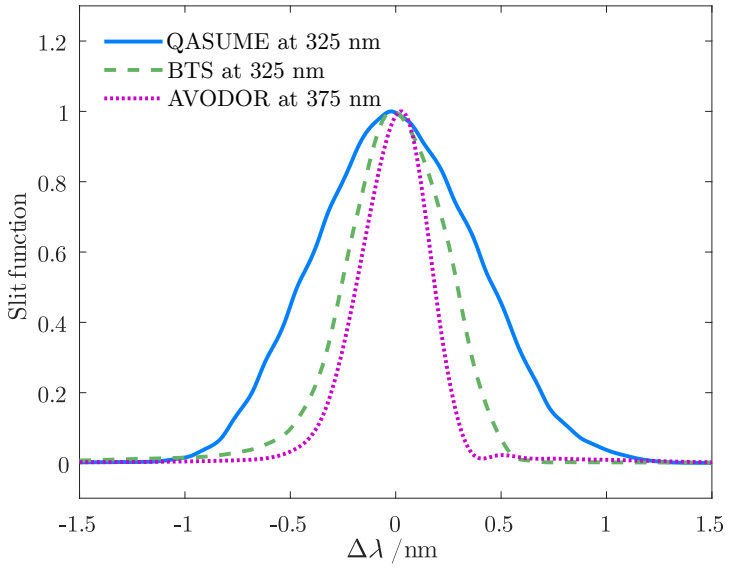

Figure 2. Slit functions, measured with narrow band lasers, for the spectroradiometers used in the Izaña campaign. The laser wavelengths are stated in legends.

3 Atmospheric model

The relationship between the terrestrial spectral irradiance $E_{\mathrm{T}}(\lambda)$ and the extra-terrestrial solar spectrum $E_{\mathrm{ext}}(\lambda)$ is defined as (Huber *et al.* (1995))

$$E_{\mathrm{T}}(\lambda) = E_{\mathrm{ext}}(\lambda) \cdot \exp\left[-\alpha_{\mathrm{O_3}}(\lambda, T_{\mathrm{eff}}) \cdot \mathrm{TOC} \cdot m_{\mathrm{TOC}} - \tau_{\mathrm{R}}(\lambda, P_0, z_0, \phi) \cdot m_{\mathrm{R}} - \tau_{\mathrm{AOD}}(\lambda) \cdot m_{\mathrm{AOD}}\right], \tag{3}$$

where $\alpha_{\mathrm{O_3}}(\lambda, T_{\mathrm{eff}})$ is the ozone absorption cross-section at the effective ozone temperature T_{eff}, $\tau_{\mathrm{R}}(\lambda, P_0, z_0, \phi)$ is the Rayleigh scattering optical depth that depends on the station pressure P_0, the station altitude z_0, and the geographic latitude ϕ.

Total ozone column TOC is the vertical ozone profile $\rho_{\mathrm{O_3}}(z)$ integrated over altitudes as

$$\mathrm{TOC} = \int_{z_0}^{z_1} \rho_{\mathrm{O_3}}(z)\,\mathrm{d}z \tag{4}$$

from the station altitude z_0 to the top-of-the-atmosphere altitude z_1. The relative air mass of the ozone layer with the Earth curvature taken into account can be expressed as

$$m_{\mathrm{TOC}} = \frac{1}{\cos\left[\arcsin\left(\frac{R}{R+h_{\mathrm{eff}}} \cdot \sin\theta\right)\right]}, \tag{5}$$

where θ is the incident solar zenith angle between vacuum-to-air interface that is a function of the local time, date, and geographic coordinates (Meeus (1998); Reda and Andreas (2008)). Parameter h_{eff} is the altitude of the ozone layer from the

Atmos. Meas. Tech. Discuss., https://doi.org/10.5194/amt-2017-403
Manuscript under review for journal Atmos. Meas. Tech.
Discussion started: 5 February 2018

Atmospheric Measurement Techniques Discussions

ground, and R is the radius of the Earth. As the ozone and molecules creating the Rayleigh scattering are distributed at different altitudes, we calculate the relative air mass factors $m_{\mathrm{R}} \approx m_{\mathrm{AOD}}$ for Rayleigh scattering and aerosols at the altitude of 5 km (Gröbner and Kerr (2001)). The temperature dependence of $\alpha_{\mathrm{O_3}}(\lambda, T_{\mathrm{eff}})$ between 203 K and 253 K (Weber *et al.* (2016)) was interpolated by a second degree polynomial at each wavelength (Paur and Bass (1985)) as

$$\alpha_{\mathrm{O_3}}(\lambda, T_{\mathrm{eff}}) = a_1(\lambda) T_{\mathrm{eff}}^2 + a_2(\lambda) T_{\mathrm{eff}} + a_3(\lambda). \tag{6}$$

We take the Rayleigh scattering optical depth into account by the state-of-the-art model by (Bodhaine *et al.* (1999)). The aerosol optical depth (AOD) is approximated (Ångström (1964)) as

$$\tau_{\mathrm{AOD}}(\lambda) = \beta \cdot \lambda^{-\alpha}, \tag{7}$$

where constant $\alpha \approx 1.4$ is the Ångström coefficient at typical atmospheric conditions (Toledano *et al.* (2007)) and β is the extinction coefficient. The wavelength λ is expressed in units of µm.

The terrestrial spectrum $E_{\mathrm{T}}(\lambda)$ convolved by the slit function of the spectroradiometer, as shown in Fig. 2, is fitted with parameters TOC and β to the measured ground-based spectrum $E(\lambda)$. The absolute TOC level obtained varies depending on the selected least squares fitting method. We used a relative least squares fitting method (Levenberg (1944); Marquardt (1963)) as

$$S = \sum_{i=1}^{n} \left[\frac{E_{\mathrm{T}}(\lambda_i) - E(\lambda_i)}{E(\lambda_i)} \right]^2, \tag{8}$$

where S is the sum of the squared residuals to be minimized. Index $i = 1, 2, ..., n$ runs over the wavelengths of the spectral measurements. This approach is consistent with the ozone measurement with Brewer MkIII spectrophotometers (Kipp & Zonen (2015)), which are used as reference devices for ozone measurements established by the International Meteorological Organization, the Commission for Instruments and Methods of Observation (CIMO) (Redondas *et al.* (2016)). The Brewer MkIII instruments solve absolute TOC values through rearrangement of Eq. (3) and by comparing the logarithms of ratios of count rates between four wavelength channels, i.e. using the double ratio technique.

Figure 3 presents examples of measurements and modelled values for the spectroradiometers used in this work. As can be seen, the signal-to-noise ratios of the devices differ significantly from each other.

Atmos. Meas. Tech. Discuss., https://doi.org/10.5194/amt-2017-403
Manuscript under review for journal Atmos. Meas. Tech.
Discussion started: 5 February 2018

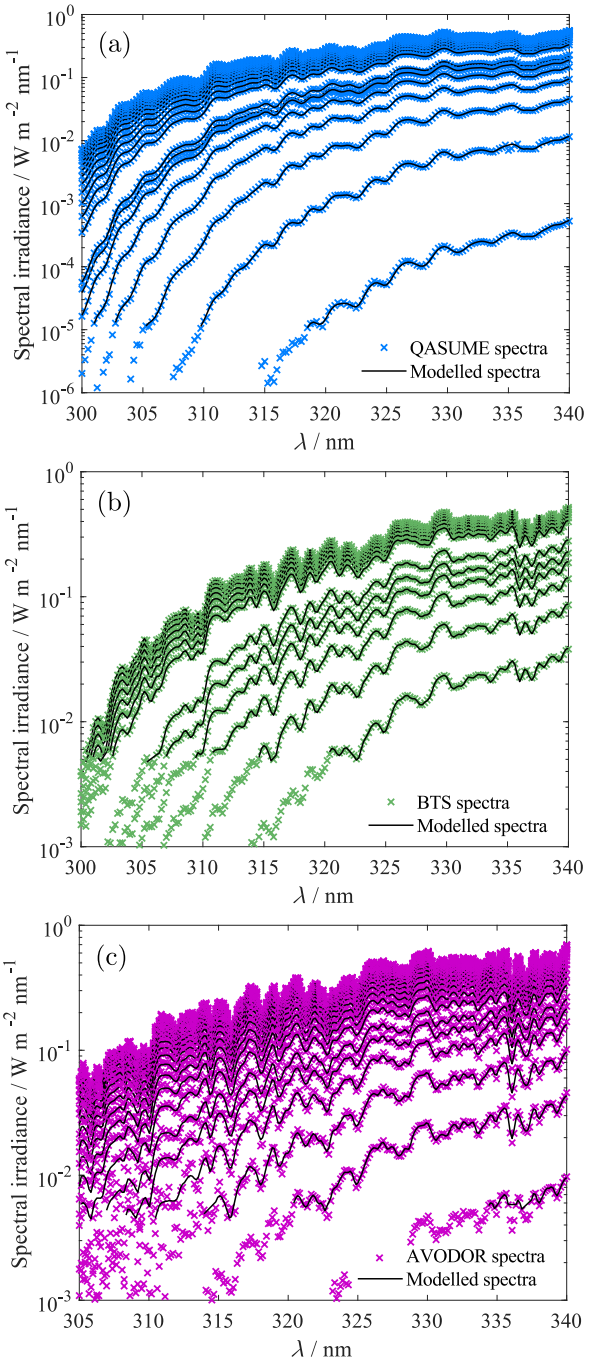

Figure 3. Examples of fitting the atmospheric model to the direct ground-based solar UV spectra for QASUME (a), BTS (b) and AVODOR (c). The coloured symbols denote measured spectra, whereas the black solid curves indicate modelled spectra.

Atmos. Meas. Tech. Discuss., https://doi.org/10.5194/amt-2017-403
Manuscript under review for journal Atmos. Meas. Tech.
Discussion started: 5 February 2018

Atmospheric Measurement Techniques Discussions

There are various ways of how to deal with noise, and the selection affects the obtained fitting results. In this work, we limit the spectral range for each device by selecting a wavelength region where the signal is above the noise floor in all measurements. Removing noisy results improves the quality of fits especially with the spectrograph type instruments AVODOR and BTS that suffer from higher stray light than QASUME. Generally, measurement results do not improve by reducing data points, and only the data that are below the noise floor should be removed. Other possibilities to deal with noise include weighting the measurement results with the inverse square of uncertainties, $u(\lambda)^{-2}$.

The shortest modelling wavelength for the monochromator based spectroradiometer (QASUME) in this work was selected to be 300 nm since the typical stray light corrections are not effective below 300 nm (Nevas *et al.* (2014)). The same limit was used for the stray light corrected BTS array spectrometer. AVODOR array spectrometer does not have any stray light correction, it shows significantly larger noise at lower wavelength, and therefore we set the short wavelength limit to 305 nm. The upper wavelength limit was set to 340 nm with all three spectroradiometers as the ozone absorption is not effective above that wavelength. In addition, a noise floor of $5{\cdot}10^{-3}$ was used for AVODOR and BTS, removing all data below this level, which affect measurements in the morning and in the evening. With QASUME, the noise floor was set to 10^{-5}. These selections can be seen in the black modelled spectra in Fig. 3.

4 Uncertainty estimation

4.1 Uncertainty model

In uncertainty analysis, the combined uncertainties are calculated with the square sum of the standard deviations of the components, i.e. their variances are summed up. If correlations of uncertainties are known, they should be taken into account. This can be carried out with the methods defined in the Guide to the Expression of Uncertainty in Measurement (JCGM 100 (2008)). In this paper, we do this for all components, where the mechanism of contributing to the uncertainty of TOC is known. However, with some of the components, we do not know exactly the mechanisms leading into correlations. With such uncertainties, we estimate the effects that possible correlations might have using a newly developed MC model described in (Kärhä *et al.* (2017a, b)).

Possible systematic deviations contained within uncertainties are reproduced using a cumulative Fourier series

$$\delta(\lambda) = \sum_{i=0}^{N} \gamma_i f_i(\lambda) \tag{9}$$

with sinusoidal base functions

$$f_i(\lambda) = \sqrt{2} \cdot \sin\left[i \left(2\pi \frac{\lambda - \lambda_1}{\lambda_2 - \lambda_1} \right) + \phi_i \right], \tag{10}$$

where index i depicts the order of complexity of the deviation (Kärhä *et al.* (2017b)), $\lambda_1 = 300$ nm or 305 nm depending on the spectroradiometer and $\lambda_2 = 340$ nm limit the wavelength range of the analysis, and the phase ϕ_i of the base function is an equally distributed MC variable between 0 and 2π. In addition, $f_0(\lambda) = 1$ is used to account for constant offset. The weights

Atmos. Meas. Tech. Discuss., https://doi.org/10.5194/amt-2017-403
Manuscript under review for journal Atmos. Meas. Tech.
Discussion started: 5 February 2018

Atmospheric Measurement Techniques Discussions

γ_i for the base functions are selected in an N-dimensional spherical coordinate system (Hicks and Wheeling (1959)) in such a way that the variance of the final error function always remains unity. The complete N-dimensional system requires orthogonal base functions, such as full periods of sine functions, to allow an arbitrary shape of deviation function $\delta(\lambda)$ with unity variance. The obtained error functions are used to distort the measured spectra $E(\lambda)$ as

$$E_{\mathrm{e}}(\lambda) = [1 + \delta(\lambda)\, u(\lambda)]\, E(\lambda)\,. \tag{11}$$

The corresponding spectral deviation is applied separately to the factors of Eq. (3), i.e., the extra-terrestrial solar spectrum, ozone absorption cross-section, and Rayleigh scattering.

Variances of the TOC values obtained by varying the weights γ_i and the phase terms ϕ_i give the desired uncertainties. Figure 4 presents how the uncertainty induced by deviation in spectral irradiance changes with increasing N. As we can see, *full* correlation with the base function $f_0(\lambda)$ at $N = 0$ causes small uncertainty to TOC. The maximum at $N = 1$ gives uncertainty for an *unfavourable* case of correlations with base functions $f_0(\lambda)$ and $f_1(\lambda)$. Cases $N = 80$ for QASUME, $N = 100$ for BTS, or $N = 125$ for AVODOR correspond to the Nyquist criterion with base functions and give the uncertainty with no spectral correlations (only noise). The obtained TOC value is affected most by spectral distortion that mimics the spectral shape of the ozone absorption that may be approximated by a slope. The first combination of constant offset and one sinusoidal function with two sign changes within the region of interest is closest to this extreme.

The ozone absorption cross-section is a direct multiplier of TOC, and thus the uncertainty in TOC is directly proportional to the deviations in the ozone absorption cross-section. Unlike the negligible effect of *full* spectral correlation in the spectral irradiance in TOC in Fig. 4, *full* correlation ($N = 0$) in the ozone absorption cross-section produces approximately the same uncertainty as *unfavourable* correlation ($N = 1$). Generally, these results cannot be known before the analysis is carried out, using a method that does not have any internal limitation to the shape of the error function $\delta(\lambda)$. In some other cases, the uncertainty extreme appears at higher N-values, e.g., $N = 3$ noted for correlated color temperature in (Kärhä *et al.* (2017b)).

One major problem in uncertainty estimation is that typically many of the correlations in spectral irradiance data are unknown. Figure 4 can be used to find limits for the uncertainties assuming different correlation scenarios. In the analysis carried out in this paper, we estimate for each uncertainty component which kind of correlations it most likely has. For this, we divide the correlation into three categories, *full*, *unfavourable*, and *random* and estimate fractions on the assortment of these correlations. *Full* indicates that error is wavelength independent such as with geometrical factors. *Random* indicates no correlation (noise). As can be seen in Fig. 4, the uncertainty caused by noise depends on the Nyquist criterion, increasing with the smaller number of base functions. *Unfavourable* indicates a spectrally varying error such as a slope that produces a large error in TOC.

Atmos. Meas. Tech. Discuss., https://doi.org/10.5194/amt-2017-403
Manuscript under review for journal Atmos. Meas. Tech.
Discussion started: 5 February 2018

Atmospheric Measurement Techniques Discussions

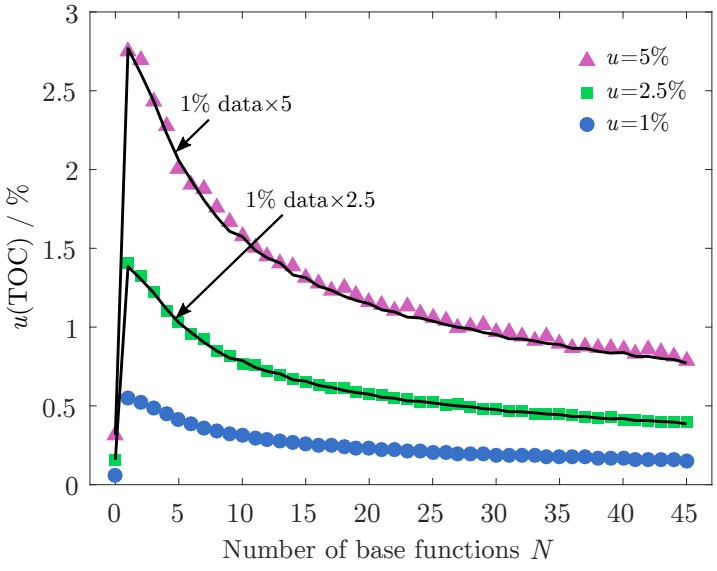

Figure 4. Uncertainties of TOC at noon as a function of the order of complexity N at three different levels of uncertainty in spectral irradiance $E(\lambda)$ at 295 nm – 340 nm with the wavelength interval of 0.5 nm indicated with symbols in the figure legend. The black solid lines obtained by multiplying the 1% uncertainties indicate the scalability of the model (Kärhä *et al.* (2017a)).

4.2 Uncertainty budget

Table 4 presents an uncertainty budget for TOC that would be obtained with the high-accuracy QASUME spectroradiometer at noon. All major uncertainty components are listed and estimated. The components stating fractions have been analysed with the new model. The other components have been solved analytically because the mechanism for the uncertainty propagating to TOC is known.

Atmos. Meas. Tech. Discuss., https://doi.org/10.5194/amt-2017-403
Manuscript under review for journal Atmos. Meas. Tech.
Discussion started: 5 February 2018

Atmospheric Measurement Techniques Discussions

Table 4. An example uncertainty budget for QASUME spectroradiometer measured at noon on the clear day of 17 September 2016. The last column states the standard deviations in $u(\mathrm{TOC})$ corresponding to each individual uncertainty component, when measuring TOC = 282 DU with the spectral range of 300 nm – 340 nm and at the solar zenith angle of 26.35°. The expanded uncertainty stated, $U(\mathrm{TOC}) = 3.7$ DU, has been obtained by multiplying the combined standard uncertainty with coverage factor $k = 2$.

Source of uncertainty	Standard uncertainty $E(\lambda)$ %	$\tau_X(\lambda) \cdot m_X$ %	Correlation *full*	*unfavourable*	*random*	$u(\mathrm{TOC})$ DU
				Fraction		
Measurement						
Radiometric calibration	0.55		$1/\sqrt{3}$	$1/\sqrt{3}$	$1/\sqrt{3}$	0.43
250 W lamp stability (one year)	0.14		1	0	0	0.02
Non-linearity	0.25		0	1	0	0.35
Stability	0.60		1	0	0	0.10
Temperature dependence	0.20		1	0	0	0.03
Measurement noise	0.20		0	0	1	0.07
Wavelength shift	0.10		0	1	0	0.14
Uncertainties related to $E(\lambda)$						
Extra-terrestrial spectrum (Gröbner *et al.* (2017))	1.00		$1/\sqrt{3}$	$1/\sqrt{3}$	$1/\sqrt{3}$	1.00
Uncertainties related to $\tau_X(\lambda) \cdot m_X$						
O_3 cross-section (Weber *et al.* (2016))		1.5	0.23	0.23	0.95	1.41
Rayleigh scattering (Bodhaine *et al.* (1999))		0.1	$1/\sqrt{3}$	$1/\sqrt{3}$	$1/\sqrt{3}$	0.09
O_3 layer altitude of 26 km, $u = 0.5$ km		(a)				0.01
Rayleigh layer altitude of 5 km, $u = 0.5$ km		(b)				0.00
Temperature of O_3 cross-section at 228 K, $u = 1$ K		(c)				0.28
Station pressure of 772.8 hPa, $u = 1.3$ hPa		(d)				0.05
					$U(\mathrm{TOC})$	**3.70**

(a) Air mass m_{TOC} varies as a function of the altitude of O_3 layer.

(b) Air mass m_{R} varies as a function of the altitude of Rayleigh scattering layer.

(c) O_3 cross-section varies as a function of temperature.

(d) Rayleigh scattering depends on the station pressure.

The uncertainties produced in TOC were obtained separately for all components, by setting other uncertainties to zero. Division of the correlation to the three categories introduced are stated for each row as fractions r_{full}, r_{unfav}, and r_{random}. For

Atmos. Meas. Tech. Discuss., https://doi.org/10.5194/amt-2017-403
Manuscript under review for journal Atmos. Meas. Tech.
Discussion started: 5 February 2018

Atmospheric Measurement Techniques Discussions

example, the ground-based spectrum $E(\lambda)$ measured is deviated with the three correlation components as

$$E_{\mathrm{e}}(\lambda) = (1 + u\ r_{full}\gamma_0 f_0(\lambda)) \cdot \left(1 + u\ r_{unfav} \sum_{i=0}^{1} \gamma_i' f_i(\lambda)\right) \cdot \left(1 + u\ r_{random} \sum_{j=0}^{N} \gamma_j'' f_j(\lambda)\right) E(\lambda)\,, \tag{12}$$

where u is the standard uncertainty of the component and γ_0, γ_i', and γ_j'' are independent MC variables.

It is worth noting that not all uncertainty components affect the spectrum $E(\lambda)$ directly, but via the exponent of Eq. (3). Corresponding formulas are used to evaluate the effect of uncertainties in extra-terrestrial solar spectrum, ozone absorption cross-section, and Rayleigh scattering. The last column in Table 4 states the standard uncertainties produced by each uncertainty component with the assumed fractions, calculated with an irradiance spectrum measured at local noon with QASUME (Hülsen *et al.* (2016)). The expanded uncertainty of the TOC, obtained as the square sum of the individual components and multiplied with coverage factor $k = 2$, for this spectral measurement is 3.7 DU (1.3%).

The QASUME spectroradiometer has a combined measurement standard uncertainty of 0.91% (Hülsen *et al.* (2016); Bernhard and Seckmeyer (1999)). Division of the radiometric calibration uncertainty to equal fractions of $1/\sqrt{3}$ is based on typical spectral correlations noted in intercomparisons (Kärhä *et al.* (2017b, 2018)). The lamp data obtained from national standard laboratories are highly accurate but also typically spectrally correlated. Due to very low noise, elements such as interpolation functions, offsets and slopes are present in the data. When the calibration is transferred further, uncertainty increases due to noise, and correlations reduce. We thus assume that in this high accuracy calibration, there are equal amounts of *fully* correlated, *unfavourably* correlated, and *uncorrelated* uncertainties included. The standard lamp used has been noted to decrease in intensity with no spectral change within the region of interest, thus the resulting uncertainty is *fully* correlated. Non-linearity may cause spectral change, as low values will be systematically distorted with respect to higher values, thus *unfavourable* correlation is assumed. Stability of the QASUME readings during a day has been noted to be wavelength independent, so is the effect of temperature. Noise contains no correlations, whereas a wavelength shift will introduce *unfavourable* correlations.

For $E_{\mathrm{ext}}(\lambda)$, we use QASUMEFTS (Gröbner *et al.* (2017)). We assume the correlation to be similar to a standard lamp, thus containing equal fractions of *full*, *unfavourable*, and *random* correlations. The QASUMEFTS is provided in air wavelengths with a step size of 0.01 nm. Otherwise, the wavelength shift due to vacuum-air interface should be corrected for the extra-terrestrial spectrum.

As the reference ozone absorption cross-section, the Serdyuchenko-Gorshelev (SG) data set given in air wavelengths with a step size of 0.01 nm, was used with 1.5% standard uncertainty (Weber *et al.* (2016)). The systematic and random uncertainties of the SG data set are given separately (Weber *et al.* (2016)). We further estimate that the systematic uncertainty given may include equal fractions of *fully* correlated and *unfavourably* correlated uncertainty. Thus, according to that we use the fractions of 0.23 for *full*, 0.23 for *unfavourable* and 0.95 for *random* correlations. *Full* correlation with a fraction of 0.23 produces a standard uncertainty of 0.96 DU, *unfavourable* correlation with a fraction of 0.23 produces a standard uncertainty of 1.01 DU and *random* correlation with a fraction of 0.95 produces a standard uncertainty of 0.22 DU. As can be seen, the ozone cross-section causes an uncertainty of 1.41 DU to TOC, and is thus the dominating component in the uncertainty. If

Atmos. Meas. Tech. Discuss., https://doi.org/10.5194/amt-2017-403
Manuscript under review for journal Atmos. Meas. Tech.
Discussion started: 5 February 2018

the fractions of correlations are not equally distributed between *full* and *unfavourable*, uncertainty in TOC does not change significantly from 1.41 DU. Fractions of 0.31 for *full*, 0 for *unfavourable*, and 0.95 for *random* correlations, cause an uncertainty of 1.33 DU in TOC. Fractions of 0 for *full*, 0.31 for *unfavourable*, and 0.95 for *random* correlations, cause an uncertainty of 1.43 DU in TOC.

Rayleigh scattering and aerosols are set at the altitude of 5 km ± 0.5 km, which influences the relative air mass m_{R} (Gröbner and Kerr (2001)). This component causes negligible uncertainty to TOC. For calculating $\tau_{\mathrm{R}}(\lambda, P_0, z_0, \phi)$, we use a model by (Bodhaine *et al.* (1999)) with 0.1% uncertainty with equal estimated fractions of correlation types. The correlation has been obtained by studying how this data deviates from the model by (Nicolet (1984)). The ozone and temperature profiles were measured with a sonde during the campaign and based on the profiles the effective altitude of the ozone layer was at 26 km ± 0.5 km at the effective temperature of 228 K ± 1 K. The effect on TOC was obtained by randomly varying the altitude with the Gaussian uncertainty distribution. The same applies to air pressure that was 772.8 hPa with a standard uncertainty of 1.3 hPa. The effect of temperature on TOC was obtained by randomly varying the temperature with its standard uncertainty of 1 K. Varying temperature systematically changes the spectral ozone absorption cross-section according to Eq. (6).

5 Results and discussion

The calculated TOC values obtained by the three different spectroradiometers on 17 September 2016 are presented in Fig. 5. Expanded uncertainties of the TOC values calculated are stated in DU as error bars. Measurement results of Brewer spectrophotometer #183 used as a reference in the intercomparison have been included in Fig. 5 as well.

Atmos. Meas. Tech. Discuss., https://doi.org/10.5194/amt-2017-403
Manuscript under review for journal Atmos. Meas. Tech.
Discussion started: 5 February 2018

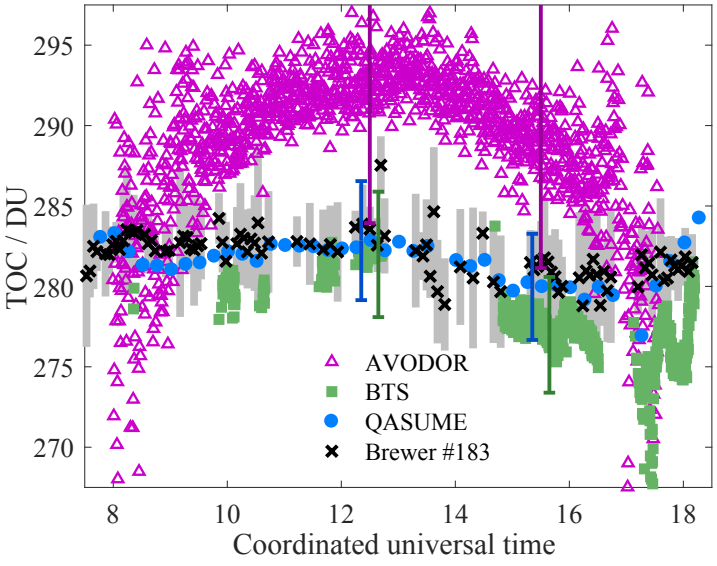

Figure 5. Derived total ozone columns with expanded uncertainty bars ($k = 2$) for QASUME (300 nm – 340 nm, noise floor of 10^{-5}), BTS (300 nm – 340 nm, noise floor of $5 \cdot 10^{-3}$), and AVODOR (305 nm – 340 nm, noise floor of $5 \cdot 10^{-3}$). The TOC measured with the Brewer #183 is plotted as black crosses with grey thick uncertainty bars ($k = 2$).

The uncertainty budget used for QASUME was presented in Table 4. For AVODOR and BTS, the components related with measurement were 2.94% and 1.24% as shown in Tables 2 and 3. For BTS, the uncertainty was distributed between correlations as follows: 0.95% for *full*, 0.62% for *unfavourable*, and 0.50% for *random* correlations. For AVODOR, the uncertainty was distributed as 1.41% for *full*, 1.35% for *unfavourable*, and 2.19% for *random* correlations. The uncertainty due to calibration was 0.8% for BTS (Zuber *et al.* (2017a)) and 2.5% for AVODOR. AVODOR has problems with noise, thus, half of the uncertainty was assumed to be *uncorrelated*. Non-linearity was assumed to be 0.5% for AVODOR and 0.4% for BTS. Measurement noise introduced uncertainties of 1.3% and 0.2% to AVODOR and BTS, respectively. With BTS, stability of the lamp was 0.2%, stability of the device was 0.8% and temperature sensitivity was 0.1%.

The relative uncertainties of the TOC values obtained with the three instruments are shown in Fig. 6. The expanded uncertainties of the TOC data sets at noon are 3.7 DU (1.3%) for the QASUME spectroradiometer, 3.7 DU (1.3%) for the BTS spectroradiometer, and 9.3 DU (3.3%) for the AVODOR spectroradiometer. The uncertainties are generally higher at noon, as the uncertainty of measurement influences more with lower air mass.

It is of interest to compare the obtained uncertainties with values assuming no correlations. If we neglect correlations, i.e., we assume the fractions in Table 4 to be 0 for the *full* and *unfavourable* correlations and 1 for the *random* correlation, and run the simulations with the spectrum measured at noon, we obtain $U_{\mathrm{QASUME}} = 1.1$ DU (0.4%), $U_{\mathrm{BTS}} = 1.1$ DU (0.4%), and $U_{\mathrm{AVODOR}} = 3.3$ DU (1.2%). These values are on average a factor of 3 lower than the uncertainties accounting for correlations. This analysis assumes random noise only. A typical practice in an analysis like this is to add a component introduced by the standard deviation of the fit to the uncertainty. The standard uncertainty to be added to the TOC because of this standard

Atmos. Meas. Tech. Discuss., https://doi.org/10.5194/amt-2017-403
Manuscript under review for journal Atmos. Meas. Tech.
Discussion started: 5 February 2018

Atmospheric Measurement Techniques Discussions

deviation is 0.28 DU with QASUME, 0.74 DU with BTS and 2.45 DU with AVODOR, raising the corresponding total expanded uncertainties to 1.3 DU (0.4%), 1.8 DU (0.7%), and 5.90 DU (2.1%).

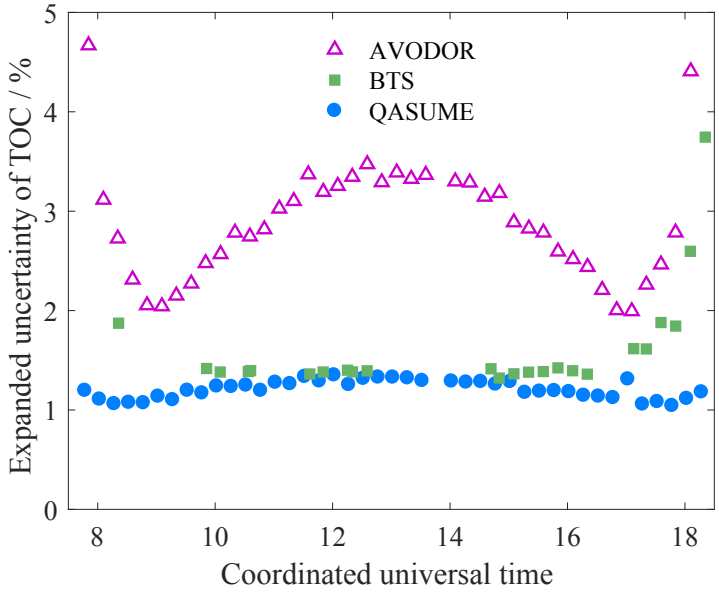

Figure 6. Relative expanded uncertainties of the total ozone columns derived from QASUME, BTS, and AVODOR spectra.

Looking at the absolute values of TOC in Fig. 5, we may conclude that the results of QASUME and Brewer #183 are in excellent agreement. Also the results of BTS are in good agreement at noon, but start deviating slightly at higher zenith angles. The ozone levels measured by the AVODOR spectroradiometer have a large discrepancy of 10 DU at noon and a strong dependence on the solar elevation angle. The offset of the AVODOR, and the angular structure of both spectrographs, are due to spectral correlations present in the measurements. Stray light and non-linearity cause systematic effects in measurements, which most likely explain the dependence as a function of solar zenith angle. Stray light that affects results at large solar zenith angles has not been accounted for in the uncertainty analysis due to lack of information. Proper correction and estimation of the uncertainty due to stray light would require the stray light correction matrix (Nevas *et al.* (2014)) to be measured.

The 10 DU deviation of the AVODOR at noon is large, barely within the calculated uncertainty, so it was studied in more detail. It appears that the reason is a systematic deviation either in the linearity, stray light properties, or the calibration of the device. Further information may be obtained by studying the AOD that is the other term to be fitted in addition to TOC, plotted for the three instruments in Fig. 7(a). The aerosol optical depth is a property of the atmosphere, and thus all the instruments should see the same AOD spectrum when the measurements are carried out at the same place and time. This applies more or less to QASUME and BTS, but for AVODOR $\tau_{\mathrm{AOD}}(\lambda)$ does not resemble AOD anymore.

Atmos. Meas. Tech. Discuss., https://doi.org/10.5194/amt-2017-403
Manuscript under review for journal Atmos. Meas. Tech.
Discussion started: 5 February 2018

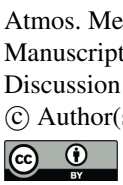

Atmospheric Measurement Techniques Discussions

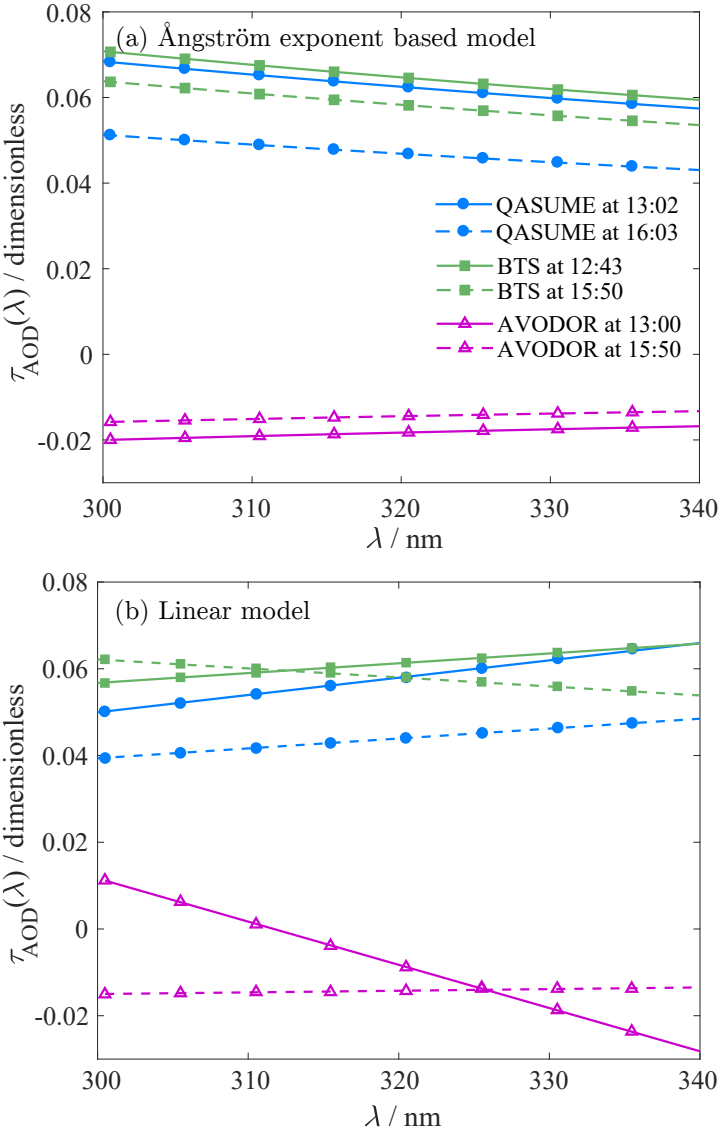

Figure 7. Aerosol optical depth (AOD) spectra obtained from QASUME, BTS, and AVODOR data sets by fitting, using the Ångström exponent based AOD model of Eq. (7) in (a) and the linear AOD model of Eq. (13) in (b). The solid lines indicate AOD at noon. The dashed lines are for a later measurement with the larger zenith angle.

There is a systematic wavelength dependent error in the measured spectra and the modelling algorithm tries to minimize this with AOD. The phenomenon was further studied by changing the $\tau_{\mathrm{AOD}}(\lambda)$ of (Ångström (1964)) to a linear model as

$$\tau_{\mathrm{AOD}}(\lambda) = a \cdot (\lambda - 340\ \mathrm{nm}) + b \tag{13}$$

Atmos. Meas. Tech. Discuss., https://doi.org/10.5194/amt-2017-403
Manuscript under review for journal Atmos. Meas. Tech.
Discussion started: 5 February 2018

Atmospheric Measurement Techniques Discussions

where λ is the wavelength in nm, and both a and b are fitting parameters in addition to TOC. This model is more parametrised so it can cause more changes to match with the measured spectra. Changing the AOD model had a drastic effect on the AVODOR results. The absolute TOC values dropped by several per cent, and were in much better agreement with the other devices. Also the dependence of the TOC on the zenith angle improved. However, $\tau_{\mathrm{AOD}}(\lambda)$ obtained did not describe the physical attenuation by aerosols anymore, which can be seen as the changing slopes in Fig. 7(b), indicating that the AOD part of the model was correcting for something different than AOD.

6 Conclusions

In this work, we introduced one possible way to take into account spectral correlations in the uncertainties of the atmospheric ozone retrieval and estimated the TOC uncertainties obtained from the spectral data of three different spectroradiometers, measured at the Izaña campaign. It should be noted that the method proposed has a drawback that the unknown correlations have to be approximated based on experience. However, the method has merits in estimating the order of magnitude of possible uncertainties accounting for correlations. The typical assumption made, that uncertainties are spectrally uncorrelated, is just an assumption as well, and in many cases not valid. The uncertainty values obtained with the new model are higher than the uncertainties obtained with the traditional method neglecting correlations because some of the major uncertainty components may contain systematic spectral deviations. These results demonstrate the importance of accounting for correlations. If their origins and magnitudes are known, they can be accounted for precisely using methods of (JCGM 100 (2008)).

The new model uses the similar approach to our previously developed MC uncertainty model for correlated colour temperature (CCT) (Kärhä *et al.* (2017b)). In the article, we demonstrated the use of the model for calculating the CCT of a Standard Illuminant A. For Standard Illuminant A, the case representing uncertainty with *unfavourable* correlations in CCT was found at $N = 3$. On the contrary, for ozone retrieval the deviation at $N = 1$ base functions produces the largest uncertainty, which is in a way trivial compared with CCT. The use of a set of sine functions as base functions was originally developed for the more complicated situation of CCT where it was not known where the *unfavourable* uncertainty would be. When we now have analysed the situation, the case of *unfavourable* correlations in the ozone retrieval could as well be modelled e.g. using the derivative of the solar UV irradiance, a derivative of the ozone cross-section, or a simple slope as the deviation function mimicking *unfavourable* correlations, which would simplify the model.

The behaviour of the AVODOR spectroradiometer is a good example about what spectral correlations in uncertainties due to systematic error components may cause. With AVODOR, the results deviate 10 DU from the other instruments, which is more than the uncertainties assuming no correlations predict, 5.9 DU. Our approach gives uncertainty of 9.3 DU which barely covers the noted deviation. It was also noted that the modelling of AOD does not work with this device, because the part of the model meant for correcting AOD starts to correct for the systematic error in the measurement results, and thus affects the TOC obtained. Spectroradiometers to be used for deriving TOC should be better with respect to systematic effects. Thus, they should be corrected for stray light and linearity, and care should be taken in their calibration not to leave systematic errors in their responsivity. The QASUME and BTS spectroradiometers are significantly better in this respect.

Acknowledgements. Peter Sperfeld from PTB is acknowledged for measuring and providing the BTS data set. Alberto Redondas and all personnel from Izaña Atmospheric Research Center, AEMET, Tenerife, Canary Islands, Spain, are acknowledged for measuring and providing the Brewer #183 data set and the environmental parameters such as the sonde data. A.V. is grateful for the incentive grant by the Emil Aaltonen Foundation, Finland. This work has been supported by the European Metrology Research Programme (EMRP) within the joint research project ENV59 "Traceability for atmospheric total column ozone" (ATMOZ). The EMRP is jointly funded by the EMRP participating countries within EURAMET and the European Union.

References

ATMOZ campaign, 2016, URL = http://http://rbcce.aemet.es/2015/11/24/atmoz-intercomparison-campaign-at-izana-tenerife-september-2016/

Ångström A.: The parameters of atmospheric turbidity, Tellus, 16, 64–75, 1964.

Bernhard G. and Seckmeyer G.: Uncertainty of measurements of spectral solar UV irradiance, J. Geophys. Res., 104, 14321–14345, 1999.

Bodhaine B. A., Wood N. B., Dutton E. G., and Slusser J. R.: On Rayleigh Optical Depth Calculations, J. Atmos. Oceanic Tech., 16, 1854–1861, 1999.

Fragkos K., Bais A. F., Balis D., Meleti C., and Koukouli M. E.: The Effect of Three Different Absorption Cross-Sections and their Temperature Dependence on Total Ozone Measured by a Mid-Latitude Brewer Spectrophotometer, Atmosphere-Ocean, 53, 19–28, 2015.

Gardiner B. G., Webb A. R., Bais A. F., Blumthaler M., Dirmhirn I., Forster P., Gillotay D., Henriksen K., Huber M., Kirsch P. J., Simon P. C., Svenoe T. , Weihs P., and Zerefos C. S.: European intercomparison of ultraviolet spectroradiometers, Environ. Technol., 14, 25–43, 1993.

Gröbner J. and Kerr J. B.: Ground-based determination of the spectral ultraviolet extraterrestrial solar irradiance: Providing a link between space-based and ground-based solar UV measurements, J. Geophys. Res., 106, 7211–7217, 2001.

Gröbner J., Kröger I., Egli L., Hülsen G., Riechelmann S., and Sperfeld P.: The high resolution extra-terrestrial solar spectrum determined from ground-based solar irradiance measurements, Atmos. Meas. Tech., 10, 3375–3383, 2017.

Gröbner J., Schreder J., Kazadzis S., Bais A. F., Blumthaler M., Görts P., Tax R., Koskela T., Seckmeyer G., Webb A. R., and Rembges D.: Traveling reference spectroradiometer for routine quality assurance of spectral solar ultraviolet irradiance measurements, Appl. Opt., 44, 5321–5331, 2005.

Hicks J. S. and Wheeling R. F.: An efficient method for generating uniformly distributed points on the surface of an n-dimensional sphere, Commun. ACM, 2, 17–9, 1959.

Huber M., Blumthaler M., Ambach W., and Staehelin J.: Total atmospheric ozone determined from spectral measurements of direct UV irradiance, Geophys. Res. Lett., 22, 53–56, 1995.

Hülsen G., Gröbner J., Nevas S., Sperfeld P., Egli L., Porrovecchio G., and Smid M.: Traceability of solar UV measurements using the QASUME reference spectroradiometer, Appl. Opt., 55, 7265–7275, 2016.

JCGM 100, Evaluation of measurement data – Guide to the expression of uncertainty in measurement (ISO/IEC Guide 98–103), 2008.

Kerr J. B. and McElroy C. T.: Evidence for large upward trends of ultraviolet-B radiation, Science, 262, 1032–1034, 1993.

Kipp & Zonen: Brewer MkIII Spectrophotometer, Operator's manual Rev F, 2015.

Komhyr W. D., Mateer C. L., and Hudson R. D.: Effective Bass-Paur 1985 ozone absorption coefficients for use with Dobson ozone spectrophotometers, J. Geophys. Res., 98, 20451–20465, 1993.

Kärhä P., Vaskuri A., Gröbner J., Egli L., and Ikonen E.: Monte Carlo analysis of uncertainty of total atmospheric ozone derived from measured spectra, AIP Conference Proceedings, 1810, 110005, 2017a.

Kärhä P., Vaskuri A., Mäntynen H., Mikkonen N., and Ikonen E.: Method for estimating effects of unknown correlations in spectral irradiance data on uncertainties of spectrally integrated colorimetric quantities, Metrologia, 54, 524–534, 2017b.

Kärhä P., Vaskuri A., Pulli T., and Ikonen E.: Key comparison CCPR-K1.a as an interlaboratory comparison of correlated colour temperature, Proc. of the 13th Int. Conf. on New Developments and Applications in Optical Radiometry (NEWRAD 2017), Tokyo, Japan, 13 – 16 June 2017 (accepted for publication), 2018.

Levenberg K.: A method for the solution of certain non-linear problems in least squares, Quart. Appl. Math., 2, 164–168, 1944.

Marquardt D. W.: An Algorithm for Least-Squares Estimation of Nonlinear Parameters, J. Soc. Indust. Appl. Math., 11, 431–441, 1963.

McKenzie R. L., Aucamp P. J., Bais A. F., Björn L. O. and Ilyas M.: Changes in biologically-active ultraviolet radiation reaching the Earth's surface, Photochem. Photobiol. Sci., 6, 218–231, 2007.

Meeus J.: *Astronomical Algorithms*, 2nd Edition, (Willmann-Bell, Richmond, VA, USA), 1998.

Molina M. J. and Rowland F. S.: Stratospheric sink for chlorofluoromethanes: chlorine atom-catalysed destruction of ozone, Nature, 249, 810–812, 1974.

Nevas S., Gröbner J., Egli L., and Blumthaler M.: Stray light correction of array spectroradiometers for solar UV measurements, Appl. Opt., 53, 4313–4319, 2014.

Nicolet M.: On the molecular scattering in the terrestrial atmosphere: An empirical formula for its calculation in the homosphere, Planet. Space Sci., 32, 1467–1468, 1984.

Paur R. J. and Bass A. M.: The ultraviolet cross-sections of ozone: II. Results and temperature dependence, Atmospheric Ozone, 611–616, 1985.

Reda I. and Andreas A.: Solar Position Algorithm for Solar Radiation Applications, Technical Report NREL/TP-560-34302, Colorado, USA, Revised 2008.

Redondas A., Rodríguez-Franco J. J., López-Solano J., Carreño V., Leon-Luis S. F., Hernandez-Cruz B., and Berjón A.: The Regional Brewer Calibration Center - Europe: an overview of the X Brewer Intercomparison Campaign, WMO Commission for Instruments and Methods of Observation, 1–8, 2016.

Toledano C., Cachorro V. E., Berjon A., de Frutos A. M., Sorribas M., de la Morena B. A., and Goloub P.: Aerosol optical depth and Ångström exponent climatology at El Arenosillo AERONET site (Huelva, Spain), Q. J. R. Meteorol. Soc., 133, 795–807, 2007.

Weber M., Gorshelev V., and Serdyuchenko A.: Uncertainty budgets of major ozone absorption cross sections used in UV remote sensing applications, Atmos. Meas. Tech., 9, 4459–4470, 2016.

Zuber R., Sperfeld P., Nevas S., Sildoja M., and Riechelmann S.: A high dynamic stray light corrected array spectroradiometer for complex measurements in the UV spectral range, Proc. of the 13th Int. Conf. on New Developments and Applications in Optical Radiometry (NEWRAD 2017), Tokyo, Japan, 13 – 16 June, 2017a.

Zuber R., Sperfeld P., Riechelmann S., Nevas S., Sildoja M., and Seckmeyer G.: Adaption of an array spectroradiometer for total ozone column retrieval using direct solar irradiance measurements in the UV spectral range, Atmos. Meas. Tech. (Discussions), 2017b.